IMA Journal of Applied Mathematics (2019) **84**, 23–43
doi:10.1093/imamat/hxy047
Advance Access Publication on 21 September 2018

Game dynamic model of social distancing while cost of infection varies with epidemic burden

Samit Bhattacharyya*
Department of Mathematics, School of Natural Sciences, Shiv Nadar University, NH-91, Gautan Buddha Nagar, UP 201314 India
*Corresponding author: samit.b@snu.edu.in

and

Timothy Reluga
Mathematics Department, Pennsylvania State University, 104 McAllister Building, University Park, State College, PA 16802 USA

[Received on 13 April 2018; revised on 14 April 2018; accepted on 29 August 2018]

'Social distancing' during an infectious disease outbreak can play a major role in controlling the spread of the disease. Individuals' interests in isolating themselves however, are constrained by the inherent costs in it. Rational decision making requires comparing the cost of social distancing with the cost of being infected such as availability of the vaccines, drugs, and treatment facilities that may depend on the current epidemic burden in the community. To understanding these, we develop a differential population game model of social distancing integrating with a simple SIR model describing the disease process. Using several type of cost functions of infections, we compute the Nash equilibrium strategies under variable efficiencies of social distancing. We also derive the closed form of the analytical solution of the utility functions under a special case. Depending on the efficiency of social distancing and the functional dependence of the cost of infections, we have shown that individuals behave very rationally to isolate themselves. This information may be useful in designing the public health policies during an epidemic outbreak.

Keywords: social distancing; cost of infection; epidemiological game; nash equilibrium.

1. Introduction

Human behaviour in response to an outbreak can potentially impact the dynamics of the epidemic (Funk *et al*., 2010). Individual behaviour in the face of an outbreak can range from wearing protective masks or vaccination to more creative precautions, all of which amount to avoiding social contacts with infected individuals i.e. 'social distancing'. There has been a good number of theoretical work that addressed the impact of human behavioural interactions on the dynamics of epidemic outbreak such as influenza, HIV/AIDs, smallpox, measles, pertussis and other respiratory diseases (Del Valle *et al*., 2005; Chen, 2006; d'Onofrio & Manfredi, 2009; Reluga, 2010; Bhattacharyya & Bauch, 2010, 2011; Chen *et al*., 2011; Bauch & Bhattacharyya, 2012; Bhattacharyya *et al*., 2015). Using a simulation model, Del Valle *et al*. (2005) demonstrated that timely and rapidly reduction of individuals contact activities and other precautions are highly sensitive to the spread of the disease. Even gradual and mild behavioural changes can have a dramatic impact in slowing down an epidemic. Further research on agent-based models has argued that social distancing can arrest epidemics if started quickly and maintained for a relatively

longer period (Kelso *et al*., 2009). Social distancing can also impact the outbreak pattern such as outbreak size, duration of the outbreak or even multiple waves with relatively shorter inter-epidemic periods (Caley *et al*., 2008).

While social distancing can be an effective prevention measure to reduce the outbreak severity during an epidemic, there are many factors that influence the individual behaviour in this process (Glass *et al*., 2006; Valdez *et al*., 2012, 2013). Individuals may consider the cost of social distancing as well as the benefit when making a decision. This decision may also consider the disease prevalence in the community. Theoretical works by Reluga *et al*. (2006), Chen (2009), Buonomo *et al*. (2008) and d'Onofrio & Manfredi (2009) among others have developed inductive behavioural models to show how individual decision-making evolves depending on the disease prevalence and the cost of social distancing.

However, these models do not consider the scenarios where the costs of infection change dynamically over time. At the start of an epidemic of a new disease or virus strain, the cost of infection may be large because immunizations are not available while treatment and even disease management are uncertain. This cost may then decrease as preventive measures and treatment resources are developed. On the other hand, the cost of infection during an outbreak of a familiar disease such as seasonal influenza or cholera may become higher as the epidemic progresses because stockpiled vaccines and treatment resources become scarce. Thus, different functional dependence of infection cost have different influences on individual behavioural responses and may have non-linear impact on the disease dynamics.

We develop a differential game model, where the cost of infection is changing according to the disease prevalence. We consider linear and different non-linear functions to represent the cost of infection. In differential games, strategies are functions of time; i.e. at each point in time, a player can choose a different action. Isaacs (1999) has developed a two-player differential game theory as a complement to variational calculus and optimal control theory (Lenhart & Workman, 2007). Later Reluga & Galvani (2011) extended this idea to develop a framework of population game to vaccination. Reluga (2010) considers the same framework to analyse a simple model of social distancing. However, he assumes the cost of infection per individual is constant and that makes the model much simpler to analyse. In this paper, we employ the extension of this differential game on the social distancing with variable cost of infection that depends on the disease prevalence in the community. We use a simple Kermack–McKendrick Susceptible-Infected-Recovered (SIR) model to describe the disease process (Anderson & May, 1992) and integrate with the game model to analyse the impact of behavioural interaction on the disease dynamics. We compute the subgame perfect Nash equilibria using backward induction. A subgame perfect equilibrium is a Nash equilibrium of every subgame of the original game (Osborne, 2004). Considering the variety of cost functions, we determine the equilibrium social distancing to differentiate how individuals rationally play depending on other epidemic features and the efficiency of social distancing.

We analytically derive the equilibrium cost of social distancing that depends on the utilities of being susceptible or infected. Using numerical simulations, we explore a number of cases with this variety of cost functions and show that when the cost of infection is a decreasing function of prevalence during an epidemic, equilibrium behaviour is to concentrate on social distancing effort at the beginning and the end of the epidemic, leading to an epidemic with lower outbreak size. On the other hand, when the cost of infection increases with prevalence, individuals engage in social distancing in the beginning and continue with increasing investment as the disease progress, which again leads to a smaller outbreak. Our model analysis also shows that individuals have little involvement in social distancing if slope of the cost function of infection is high, while higher efficiency impacts on the emergence of disease by

delaying the outbreak. Thus, the variable cost of infection depending on the disease prevalence may result in different equilibrium social distancing behaviour that play an important role in epidemic size and the timing of the disease outbreak.

2. Model and assumptions

We develop a differential population game model that describes the social distancing during an epidemic. Social distancing is a process that stops or slows down the transmission of an infection in a population during an epidemic. It is characterized by individual behaviour that reduces the local contacts with other individuals in the community and lessens the chance of being infected. But, social distancing exacts some cost by hindering economic growth of the individual as well as the community. Thus, people are only likely to adopt these measures when there is enough incentive to do so. Thus, the effectiveness of implanting social distancing is interrelated with the individuals choice of strategies that in turn, accounts for the chance of infection and the associated cost including treatment.

We consider the epidemic dynamics described by a simple SIR epidemic model with susceptible (X), infected (Y) and removed (Z) states. We also assume that the epidemic is fast relative to the demographic processes so we do not consider the birth and the death process, instead we assume that the population size is constant. In most of the earlier social distancing models, infection incurs a constant cost for each individual upon infection. Here, instead we assume that the infection cost varies with the outbreak size. In other words, c_I indicates the cost per unit time for individual when the person gets infected. We explore different scenarios with variety of cost functions. For example, cost of infection either decreases or increases with increase in outbreak size and have different functional forms to describe these variation.

Individuals in the population may opt either social distancing or do nothing depending on the costs of social distancing and the cost of infection. Let c_s be the cost per unit time of individual strategy or investment in social distancing; we assume the cost of social distancing impacts the disease transmission through hyperbolic function

$$\sigma(c_s) = \frac{1}{1 + mc_s}, \tag{2.1}$$

where $m = -\sigma'(0)$ denotes the maximum efficiency of social distancing. The function $\sigma(c_s)$ may be thought of as the relative risk of infection. The relative risk of infection decreases with the increase in social distancing. It may be noted that we have no such data or studies available in the literature on how actually the efficacy of social distancing changes with the cost invested by individuals in the population. However, it is bounded below by zero, and also $\sigma(0) = 1$, when there is no investment. Thus, we have the disease model given by

$$\begin{aligned} \frac{dX}{dt} &= -\sigma(c_S)\beta XY, \\ \frac{dY}{dt} &= \beta Y\sigma(c_S)X - \gamma Y, \\ \frac{dZ}{dt} &= \gamma Y, \end{aligned} \tag{2.2}$$

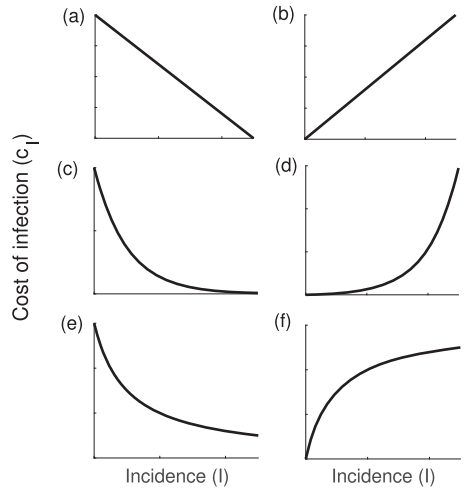

FIG. 1. Cost of infection as function of the disease incidence I. (a–b) cost function (i) $c_I(I) = a + bI$ ($b < 0$ and $b > 0$, respectively); (c–d) cost function (ii) $c_I(I) = exp(rI)$ ($r < 0$ and $r > 0$, respectively); (e–f) cost function (iii) $c_I(I)1 + \frac{bI}{k+I}$ ($b < 0$ and $b > 0$, respectively).

where β is the transmission rate and γ is the removal rate. At the start of the epidemic when there are few cases of infection ($Y(0) \sim 0$), the basic reproduction number $R_0 \sim \frac{\beta N}{\gamma}$.We assume the per unit time cost of infection depends on disease prevalence according to following functions (Fig. 1):

(i) $c_I(I) = 1 + bI, b \in \mathbb{R}$;

(ii) $c_I(I) = \exp(rI), r \in \mathbb{R}$;

(iii) $c_I(I) = 1 + \frac{bI}{k+I}, b, k \in \mathbb{R}$ and $k > 0$.

In all these cases, the cost of infection has been normalized relative to the costs of social distancing so that $c_I(0) = 1$.

We simplify our equations by letting $S = \frac{\beta}{\gamma}X$, $I = \frac{\beta}{\gamma}Y$, $R = \frac{\beta}{\gamma}Z$ and $\bar{t} = t\gamma$, so model system (2.2) reduces to

$$\begin{aligned} \frac{dS}{dt} &= -\sigma(c_S)SI, \\ \frac{dI}{dt} &= \sigma(c_S)SI - I, \\ \frac{dR}{dt} &= I. \end{aligned} \tag{2.3}$$

With these choice of units in the dimensionless model, 'time' will be measured in terms of the disease generations, and the population sizes will be measured relative to the critical population size necessary to sustain an epidemic i.e. an epidemic can only occur if $S(0) > 1$.

2.1 *Game model: Social distancing*

We construct our game model using the expected utility theory with additive payoffs including their discounting for future times. The expected utility of a strategy depends on the all future payoffs that an individual receives through its change of state over time t, and thus it is computed summing over all utility gains, and the residence cost that the individual pays throughout all states in the future times. A formal application of the utility theory in such epidemic game has been presented in Reluga & Galvani (2011).

In this present social distancing game, we formulate the behaviour submodel as a population game, where the cost of individual choice depends on the average behaviour of the population. Individuals choose their best social-distancing practises relative to the aggregate behaviour of the population as a whole. The underlined assumption of the game is that at each point in the epidemic, an individual can choose to pay a cost associated with social distancing in exchange for a reduction in the risk of infection.

The state (S, I or R) of an individual in the population over time t follows according to the disease equations (2.3), and this can be represented by a probability distribution $p(t)$, given by

$$\dot{p}(t) = Q(t; c_s, c_I)p, \tag{2.4}$$

where c_s denotes the individual's per unit time investment cost of social distancing, c_I is the per unit time cost of infection. The state transition rate matrix Q is given by

$$Q(t; c_S, c_I) = \begin{pmatrix} -\sigma(c_S)I & 0 & 0 \\ \sigma(c_S)I & -1 & 0 \\ 0 & 1 & 0 \end{pmatrix}. \tag{2.5}$$

We should note here that the cost of social distancing can be interpreted in feedback form as a function of the population's state ($c_S := c_S(S, I)$).

Now, an individual pays some cost of being a resident in one of the two state S and I, while there is no utility gain in the transition from one state to the another. So, if f is vector of the cost per unit time for residence in each state S, I or R and F is the matrix of utility gain per unit time for transition from one state to the another, then we have

$$f = \begin{bmatrix} -c_S(t) \\ -c_I(t) \\ 0 \end{bmatrix},$$

$$F = \begin{bmatrix} 0 & 0 & 0 \\ 0 & 0 & 0 \\ 0 & 0 & 0 \end{bmatrix}.$$

This gives the equation of expected value of utility $U = [U_S, U_I, U_R]$ of states $[S, I, R]$ as follows:

$$-\dot{U} = (Q - hI_3)U + \left[f^T + 1^T(F \circ Q)\right], \tag{2.6}$$

where $\circ$ represents the Hadamard product of two matrices, h is the discounting rate, I_3 is a 3×3 identity matrix and T is transpose of matrix (for reference of general form of the utility equation (2.6), see Reluga & Galvani, 2011).

Now, $u = [f^T + 1^T(F \circ Q)] = [-c_S, -c_I, 0]$, so writing the equation (2.6) in explicit form, we have

$$\begin{aligned} -\frac{dU_S}{dt} &= -hU_S - (U_S - U_I)\sigma(c_S)I - c_S, \\ -\frac{dU_I}{dt} &= -hU_I + U_R - U_I - c_I, \\ -\frac{dU_R}{dt} &= -hU_R, \end{aligned} \tag{2.7}$$

with usual parametric constraints for c_S, c_I.

Assuming $h = 0$, and also $U_R = 0$, we then have the reduced combined set of equations using (2.3) and (2.7),

$$\begin{aligned} \frac{dS}{dt} &= -\sigma(c_S)SI, \\ \frac{dI}{dt} &= \sigma(c_S)SI - I, \\ -\frac{dU_S}{dt} &= -(U_S - U_I)\sigma(c_S)I - c_S, \\ -\frac{dU_I}{dt} &= -c_I(I) - U_I, \end{aligned} \tag{2.8}$$

where $c_I(I)$ is cost of infection as described in Fig. 1.

It should be noted that the set of state equations (the first two in the model (2.8)) are calculated in forward time i.e. from initial time $t = 0$ to the final time, say $t = \infty$ (as usually the disease progression occurs from initial time $t = 0$ until it dies out) while the utility equations (the last two in the model (2.8)) are interpreted backwards from terminal time to the initial time, as we use the expected utility tomorrow to calculate the expected utility today. This allows system to frame as boundary value problem (BVP), which we discuss in the beginning of result sections.

3. Model analysis

We compute Nash equilibrium of social distancing, which is a subgame perfect equilibrium of this population game. A Nash equilibrium solution to a population game model (like the system given by (2.8) is a strategy that is a best response, even when everybody else is using the same strategy. i.e. given $U_S(t; c, c^*)$, c^* is a Nash equilibrium if for every alternative strategy c, we have $U_S(t; c, c^*) \leqslant U_S(t; c^*, c^*)$. In such games, it is the most useful to look for strategies that are equilibria, in the sense that every player's strategy is better than the alternatives, given the knowledge of their opponent's strategies. A Nash equilibrium strategy is a subgame perfect equilibrium if it is also a Nash equilibrium at the every state of the system passes through.

We execute the Nash equilibria of the system (2.8) by computing the cost of social distancing at every step in the game, which maximizes the rate of increase in the individual's expected value U_S. We represent strategies as functions in implicit feedback form. For example, $c(U_S, U_I, I)$ is the amount an

individual invests per transmission generation. So, if $c_S^* = c_S^*(U_S, U_I, I)$ is subgame perfect equilibrium, it satisfies the maximum principle, and thus we have

$$c_S^* = \text{argmax}_{c_S \geqslant 0} -(U_S - U_I)\sigma(c_S)I - c_S, \tag{3.1}$$

where c_S^* is uniquely defined by

$$c_S^* = 0, \qquad \text{if} - \sigma'(0)I(U_S - U_I) \leqslant 1, \tag{3.2}$$

$$-\sigma'(c_s^*)I(U_S - U_I) = 1, \qquad \text{otherwise.} \tag{3.3}$$

Using (2.1), we get from the last equation that

$$c_s^* = \sqrt{\frac{(U_S - U_I)I}{m}} - \frac{1}{m}. \tag{3.4}$$

It should be noted from equation (3.4) that a positive social distancing always requires $U_S > U_I$, i.e. the expected utility of susceptible is larger than that of infective, which is true as the higher utility of susceptible initiates individuals to social distancing. We have made contour plots of social distancing for different values of m in Fig. 2 using (3.4). These contours define the thresholds where equilibrium behaviour involves some social distancing.

As we mentioned earlier, the first two disease equations in the model (2.8) are calculated in forward time i.e. from time $t = 0$ to ∞, while the last two utility equations are interpreted backwards from terminal time to the initial time. The disease variables at the initial and final time points are given by $S(0) = S_0 = R_0$ (the basic reproduction ratio), $I(0) = I_0 > 0$ and $I(\infty) = 0$. The boundary point

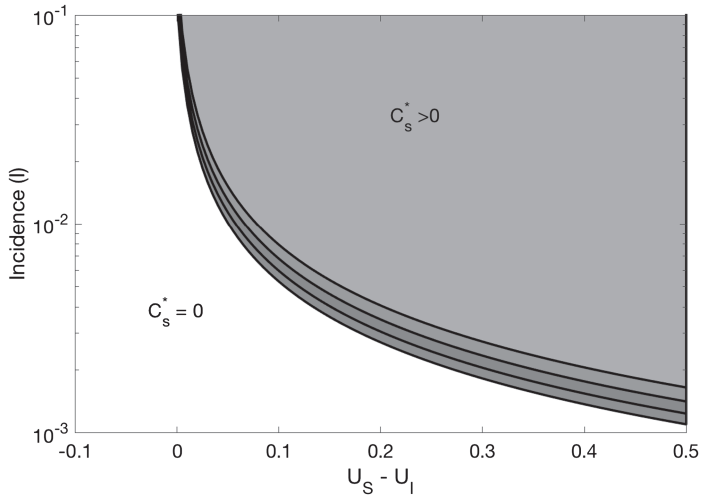

FIG. 2. Contour plot using equation (3.4) of social distancing for different values of the efficacy m (from upper to lower, curves represent for $m = 6$ to 9). Shaded region indicates the equilibrium behaviour involves some social distancing, while low values of disease prevalence initiates no social distancing (white region).

$S(\infty)$ of susceptible is unknown. On the other hand, the expected utility variable $U_S(\infty) = 0$ (as there would be no infection at $t = \infty$ and hence no incentive to be susceptible). Now $U_I(t) = -$ (cost of infection at time t)/(time spent of being infected)$= -c_I(t)/\gamma$. As there is no infection at $t = 0$ and ∞, so $c_I(0) = c_I(\infty) = 1$. So for dimensionless model, $U_I(0) = U_I(\infty) = -1$. The boundary points $S(\infty)$ and $U_S(0)$ are unknown, which eventually determine the equilibrium of the game dynamic model.

3.1 *Special case*

We can deduce the analytic form of solutions of the utility functions U_S and U_I as function of I, in a special case, where $S(0) = 0$ and $I(0) = I_0 > 0$. Here we derive a range of efficiency parameter m, when there is no social distancing. Under these conditions, $S(t) = 0$ and $I(t) = I_0 e^{-t}$, for all t. Now there is no social distancing, i.e. $c_S^* = 0$, when $mI(U_S - U_I) \leqslant 1$. With these special condition, we have the reduced form of utility equations from (2.8):

$$\begin{aligned} \frac{dU_S}{dt} &= (U_S - U_I)I \\ \frac{dU_I}{dt} &= c_I + U_I. \end{aligned} \tag{3.5}$$

We compute the special case only for the linear cost function (i) $c_I(I) = 1 + bI$, $b \in \mathbb{R}$. Incorporating the cost function and using $I = I_0 e^{-t}$, we have the final equations

$$\begin{aligned} \frac{dU_S}{dt} &= (U_S - U_I)I_0 e^{-t} \\ \frac{dU_I}{dt} &= 1 + bI_0 e^{-t} + U_I. \end{aligned} \tag{3.6}$$

We solve for U_I and then U_S separately from equations (3.6), and using the boundary conditions, and the property that both U_S and U_I are bounded for all t, we have

$$\begin{aligned} U_S &= \left(-1 + \frac{b}{2}\right) - \frac{b}{2} I_0 e^{-t}, \\ U_I &= -1 - \frac{b}{2} I_0 e^{-t}. \end{aligned} \tag{3.7}$$

We can still write U_S and U_I as function of I:

$$\begin{aligned} U_S &= \left(-1 + \frac{b}{2}\right) - \frac{b}{2} I, \\ U_I &= -1 + \frac{b}{2} I. \end{aligned} \tag{3.8}$$

The equations in (3.8) show the feedback relation of I on U_S and U_I. So, these are solutions, if $mI(U_S - U_I) = \frac{mbI}{2} \leqslant 1$, for all I, which implies $m \leqslant \frac{2}{bI_0}$. Thus, if the efficacy m of social distancing is small and

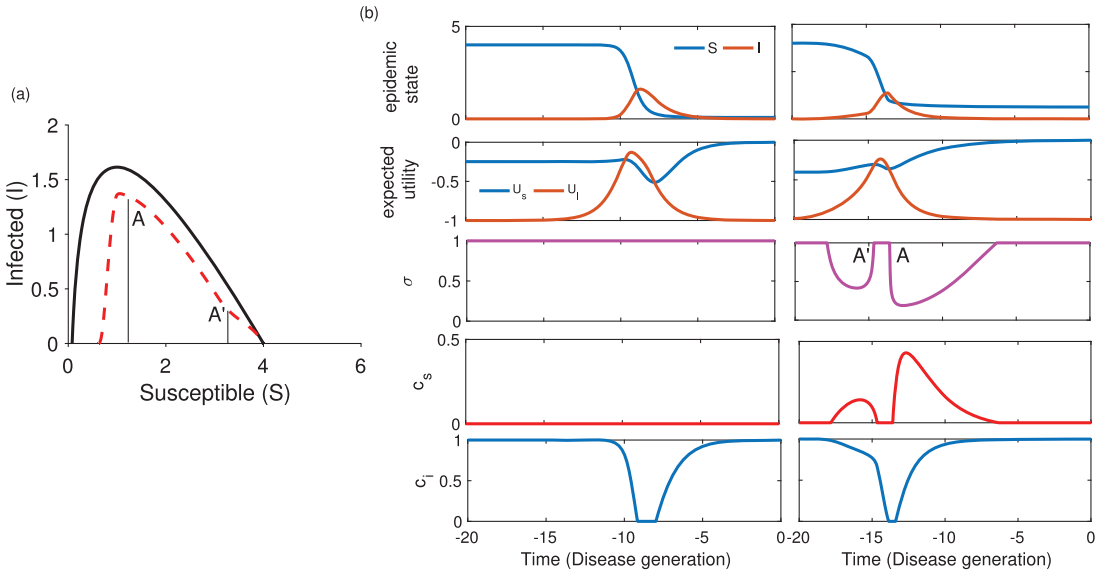

FIG. 3. Simulation of the model system (2.8) with and without social distancing with cost function (i) $c_I(I) = 1 + bI$. Figure (a) shows the $S - I$ phase plane (black curve is without social distancing and red dotted curve is with equilibrium social distancing), while (b) shows time series evolution of epidemic state, expected utility, social distancing (c_S) and cost of infection (c_I) (left panel is without social distancing and right panel shows dynamics under social distancing). Parameter values in this simulation are $R_0 = 4, m = 100, b = -0.8$. It clears from red dotted curve in (a) that there are two phases of social distancing. In fact, social distancing starts soon after disease emergence, and it continues when cost of infection becomes zero (A'). It remains zero from A' to A. Again there is social distancing when cost of infection is positive and crosses a threshold (A). This is also clear from subfigure of c_S time series in right most panel of (b). The area between the two curves in (a) indicates the difference of outbreak size due to social distancing.

less than or equal to $2/bI_0$, then individuals in population do not opt for social distancing. The solutions of U_S and U_I using the other non-linear cost functions (ii) and (iii) are complicated and we do not get such suitable range of m for positive social distancing.

4. Results

In this differential population game model (2.8), susceptible population $S(t)$ is known from the beginning at $t = 0$, but the expected utility $U_S(t)$ of being susceptible is known from future time, say $t = \infty$. We define this system as a BVP, where the boundary conditions $S(0), I(0), U_I(0), I(\infty), U_S(\infty)$ and $U_I(\infty)$ are known, but $S(\infty)$ and $U_S(0)$ are unknown. Here we set it to a problem of scalar root finding for $S(\infty)$ to match the given susceptible population at the beginning, i.e. $S(0)$. Hence, starting with arbitrary $S(\infty)$ we use the backward integration in time to compute the solution trajectories and over repeated execution we find the scalar root to match given $S(0)$. This gives the trajectories for all disease and expected utility variables from $t = 0$ to ∞ that determine the Nash strategy of social distancing. We use MATLAB R2017b to simulate the model and perform the computations for all three cost functions c_I. The code may be available from authors upon request.

(i) Cost of infection $c_I = 1 + bI$

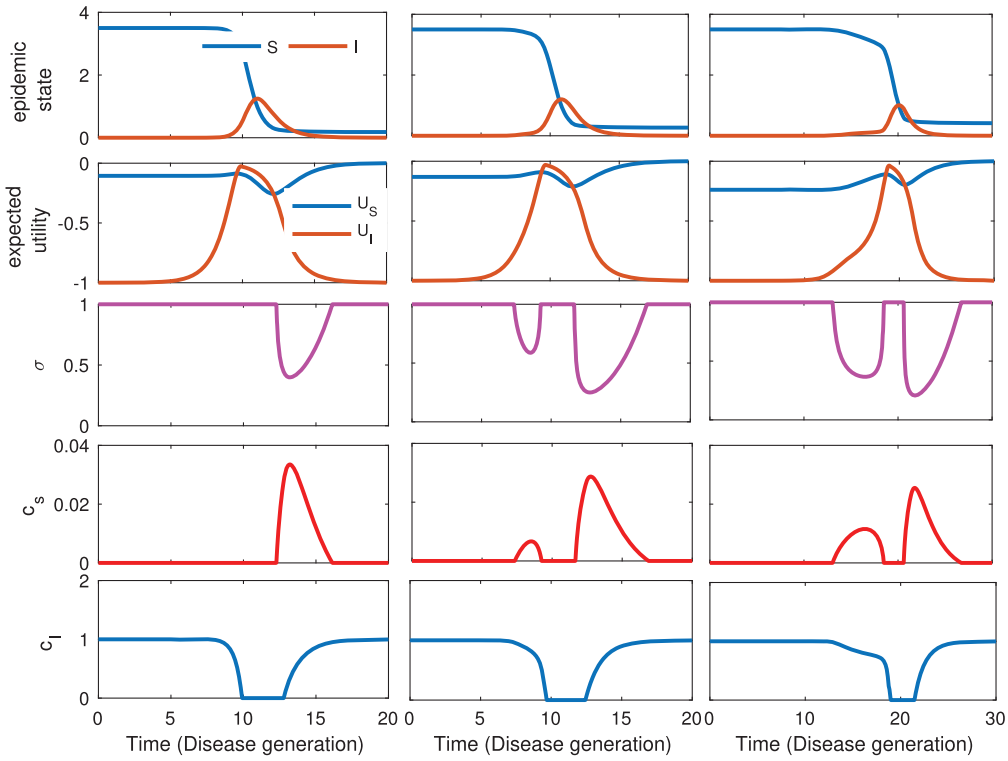

FIG. 4. Plot of time series obtained from simulation of the model equations (2.8) under different values of maximum efficiency (m) of social distancing with linear cost function (i) $c_I(I) = 1 + bI \;\; b = -2.8$. Leftmost vertical panel with $m = 45$, middle one with $m = 105$ and rightmost vertical panel figures with $m = 150$. The figure shows equilibrium social distancing behaviour (depicted by the fourth horizontal panel from top), reduction of transmission (by third horizontal panel) and change in expected utility (indicated by second horizontal panel). Higher values of efficiency (m) increases cumulative social distancing indicated by the area of the curve under $c_S > 0$, which determines substantial reduction in the transmission of infection (σ) from left to right.

Individual investment in social distancing depends on the cost of infection (henceforth, COI) and the efficiency of social distancing in isolation to protect from the infection. From (2.1), the maximum efficiency of social distancing is m. As the COI $c_I = 1 + bI$, we have

$$\text{Cost of infection per generation} = \frac{c_I}{m} = \frac{1}{m} + \frac{b}{m} I. \tag{4.1}$$

Hence, maximum COI per generation is $1/m$ in absence of linear dependence of the cost function, i.e. when $b = 0$. Thus, individuals would have to invest at least $1/m$ of the cost of infection per disease generation to totally isolate themselves, which indicates that fewer than m generations of total isolation are practical. When the cost function is dependent on the disease incidence, i.e.,$b \neq 0$, the cost per generation decreases or increases with a probability proportional to b/m depending on $b < \text{or} > 0$, respectively. With higher values of I the investment cost is zero, when $b < 0$. This indicates that there would be no incentive of social distancing when there is high prevalences and COI per generation decreases with the disease incidence.

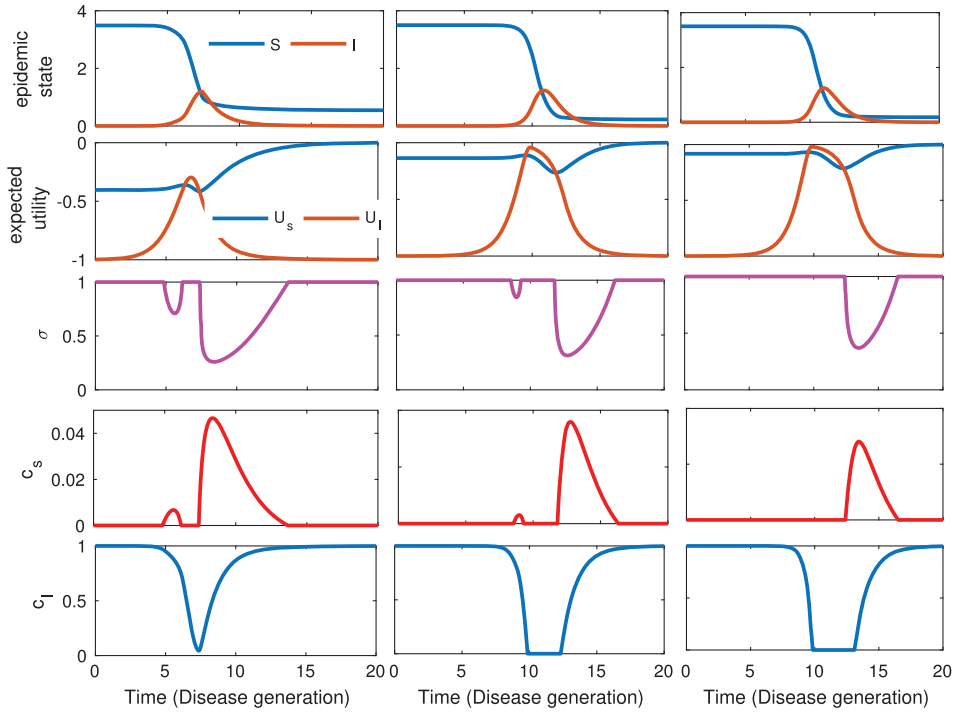

FIG. 5. Plot of time series obtained from simulation of the model equations (2.8) under different values of slope (b) of cost function $c_I(I) = 1 + bI$ with constant efficiency of social distancing $m = 45$. Leftmost vertical panel with $b = -0.8$, middle one with $b = -1.8$, and rightmost vertical panel figures with $b = -2.8$. Individuals' investment in social distancing decreases (σ) (from left to right) as the slope b increases. Thus, individuals pays low cost in social distancing while cost of infection largely decreases due to incidence.

An example of equilibrium strategy with and without social distancing is portrayed in Fig. 3, when the cost of infection is decreasing with incidence, i.e. $b < 0$. While the susceptible population $S(0)$ is at 4 and the infected population starts increasing (Fig. 3(a) and the right panel of (b)), social distancing emerges and it continues up to the point A'. At this point, the COI per generation in (4.1) is very low and there is no incentive to invest in social distancing. So, individuals do not engage in social distancing. It again emerges, when the disease burden is low and COI per generation starts increasing (denoted by A). However, low susceptible population density leads steep decline of the red dotted curve indicating rapid disease die out in the system. Thus, the difference in the areas between the black solid and the red dotted curve in Fig. 3(a) indicates the effect of social distancing on the dynamics of the disease in this differential game model.

There are three parameters that interact with each other to impact COI per generation in (4.1): the maximum efficiency m of the social distancing, the slope b of the cost of infection and the basic reproduction rate R_0. The dynamics of social distancing and its feedback on the disease prevalence in the community entirely depend on how these three parameters interplay with each other. So, we perform a scenario analysis in regime of these three parameters b, m and R_0 to compare the effect of these parameters on the system.

Figure 4 depicts the dynamics at different values of m for fixed $b = -2.8$. The efficiency parameter m has non-linear effect on the COI per generation. Higher values of m decreases the maximum COI

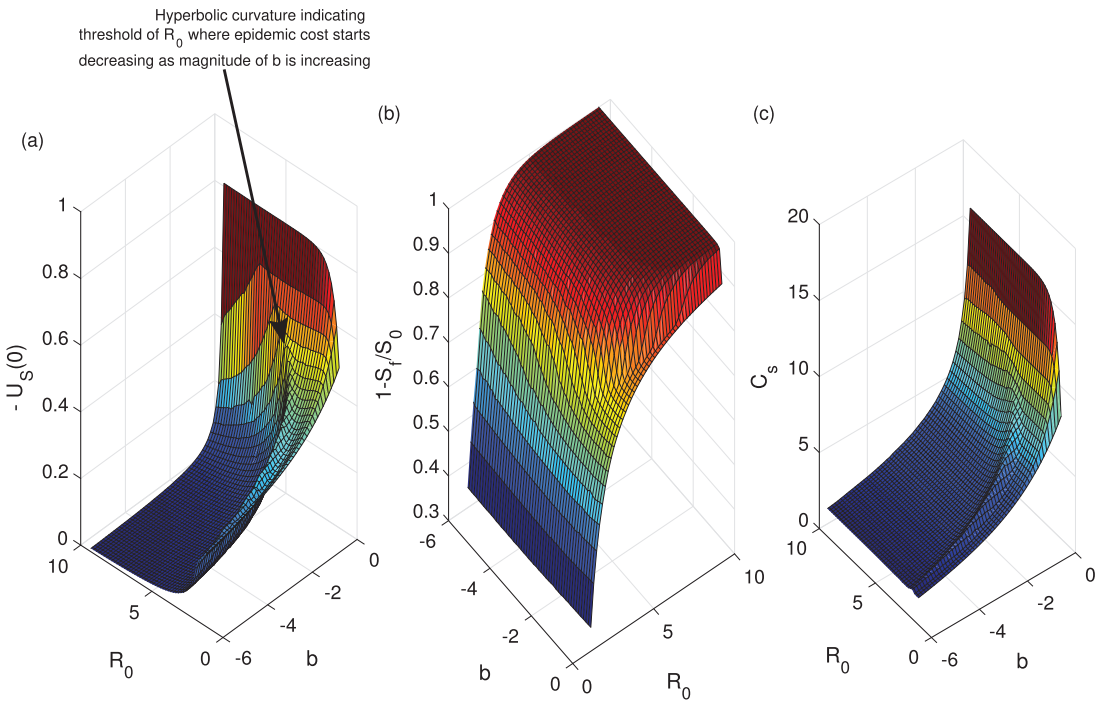

FIG. 6. (a) Per capita epidemic cost $-U_S(0)$, (b) cumulative outbreak size $(1 - S_f/S_0)$, S_0 and S_f are initial and final susceptible size), (c) social distancing cost (area under the c_s curve) for different R_0 and the slope b of the linear cost function (i) $c_I = 1 + bI$. The per capita epidemic cost (Left most panel) increases with R_0 when $b = 0$. At higher magnitude of b, initially the epidemic cost increases, but then rapidly decreases along a hyperbolic curve as R_0 decreases. A similar pattern is also observed in social distancing cost indicated in (c).

per generation, but at the same time it also reduces the influence of incidence population I on COI per generation. However, the effective COI per generation increases with increase in m when $b < 0$, and thus individuals require investing more cost in social distancing to totally isolate themselves to protect from infection. This is reflected in the Fig. 4 from the left to right panel exhibiting substantial reduction of the transmission of infection (σ). The dynamics of social distancing is also biphasic with higher values of m, implying that individuals engage in social distancing behaviour in the beginning and the end of the disease outbreak as indicated in Fig. 3. This is due to the fact that COI per generation decreases to such a low level at higher disease incidence that there is no incentive for social distancing and individuals thus refrain from the same.

There is opposite effect on the dynamics of social distancing if we increase the magnitude of slope b, ($b < 0$) at some fixed efficiency m. We consider $m = 45$ throughout and simulate the model for three values of slope b, say $b = -0.8, -1.8$, and -2.8. Higher magnitude of b reduces the effective COI per generation by increasing the effect of infected population density, and so amount of social distancing reduces as we increase the magnitude of b (Fig. 5). Also, social distancing is biphasic as seen earlier. Thus, our model shows that when the cost of infection is a decreasing function of prevalence during an epidemic, equilibrium behaviour is to concentrate on social distancing effort at the beginning and the end of the epidemic, leading to an epidemic with lower outbreak size.

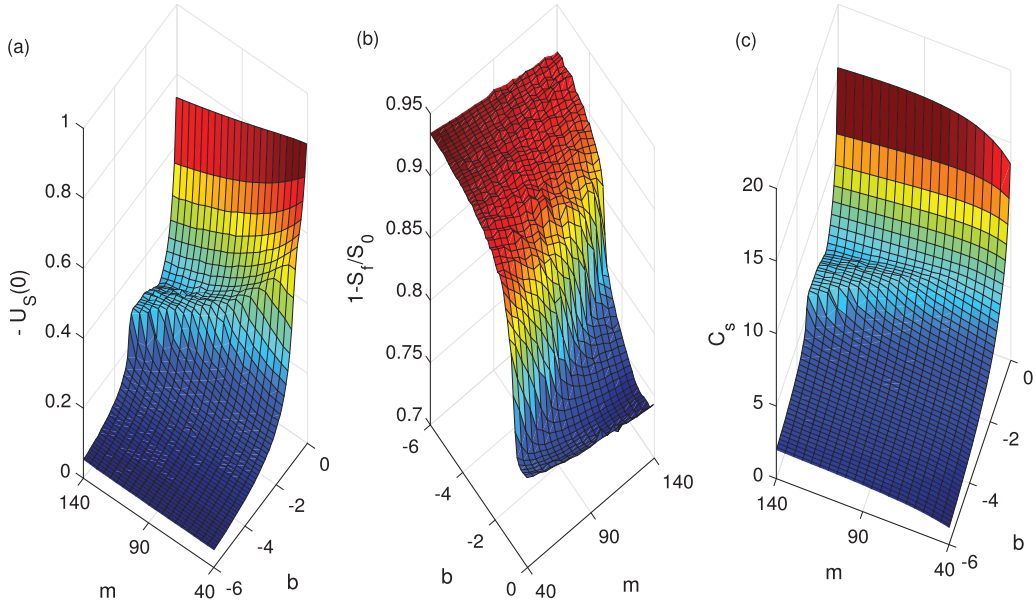

FIG. 7. (a) Per capita epidemic cost $-U_S(0)$, (b) cumulative outbreak size, (c) social distancing cost (area under the c_s curve) for different slope b of the linear cost function (i) $c_I = 1 + bI$ and maximum efficiency m of social distancing (equation (2.1)). The efficiency m does not have much influence on the epidemic cost unless there is a substantial dependence of COI on disease prevalence. As it is observed, with higher values of b, increase in m decreases the epidemic cost (leftmost panel). A similar pattern is observed in social distancing cost (rightmost panel).

The per capita cost of an epidemic $-U_S(0)$ is also dependent on the COI per generation in (17). In Fig. 6(a), we draw the epidemic cost against R_0 and the slope parameter b. As seen in Fig. 6(a), the per capita epidemic cost is increasing with the increase in R_0, when cost of infection c_I does not depend on incidence, i.e. $b = 0$. Once the cost of infection depends on incidence with $b < 0$, the epidemic cost $-U_S(0)$ increases initially, but rapidly decreases as the basic reproduction ratio R_0 crosses some threshold. This threshold of R_0 however increases along a hyperbolic curve in the plane of R_0 and b as the magnitude of b decreases. Higher R_0 increases the incidence, and that increases the per capita epidemic cost, even when $b = 0$. However, the COI per generation decreases when $b < 0$ and it becomes negligible with higher magnitude of R_0 and slope b, so the per-capita epidemic cost is reduced to zero.

As individuals investment in social distancing depends on COI per generation, the social distancing also exhibits a similar pattern (Fig. 6(c)). The outbreak size $1-S_f/S_0$, (where S_0 is the initial susceptible population and S_f is the final susceptible population when disease dies out) however increases with R_0, but comparatively to a reduced level at lower b due to social distancing (Fig. 6(b)). Thus, basic reproduction ratio R_0 and the slope b of the linear cost function c_I determine the equilibrium social distancing and total disease prevalence in the system.

In contrast, the efficiency m does not have much influence on the epidemic cost unless there is substantial dependence of COI per generation on the disease prevalence (Fig. 7). As we observe, the increase of m decreases the per capita epidemic cost at higher values of magnitude of b (Fig. 7(a)). As individuals investment in social distancing depends on COI per generation, a similar pattern is observed in equilibrium social distancing (Fig. 7(b)).

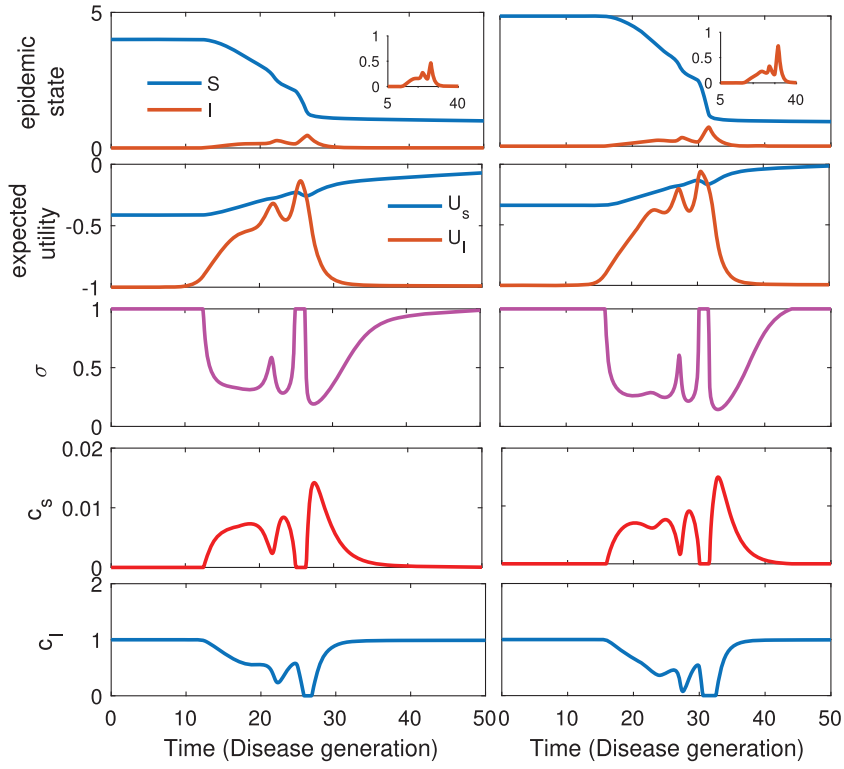

FIG. 8. Dynamics of disease and social distancing, when maximum efficiency m of social distancing is relatively higher. The left panel exhibits with $m = 300$, and right panel describes for $m = 400$. In both simulations, we consider the linear cost function (i) $c_I = 1 + bI$ and $b = -2.8$. The figure in inset is the magnified version of disease incidence I, which shows multiple small and large outbreaks. Due to higher efficacy, a little effort in social distancing induces a bigger change in the disease transmission, which in turn induces higher reduction in the prevalence. However, it reduces the incentive of social distancing as well, and so again outbreak occurs.

Social distancing during disease emergence may induce multiple outbreaks. Caley *et al.* (2008) have shown that social distancing during influenza epidemic in Sydney in 1919 led to multiple waves. They have quantified the amount of social distancing that led to the particular size and duration of the outbreak. A similar characteristic we have seen in our model analysis (Fig. 8). With higher values of m, the efficiency of social distancing increases and hence COI per generation in (17) decreases. Individuals adopt social distancing as soon as the disease emerges. This however leads to a lower infection that reduces the COI per generation and so there is no incentive for social distancing. Again it emerges as the disease prevalence starts increasing. The outbreak size and its duration depends on specific parameter values. Thus, multiple outbreaks seem to be a common phenomenon due to social distancing in the face of an outbreak.

We also analyse the dynamics of disease and social distancing when cost function is linear $c_I = 1 + bI$ and $b > 0$. This implies that the cost of infection increases as the infected population increases and thus COI per generation in (4.1) always increases with the incidence. So, it always involves social distancing behaviour when $b > 0$ (Fig. 9). However, the increase in the efficiency m will decrease the

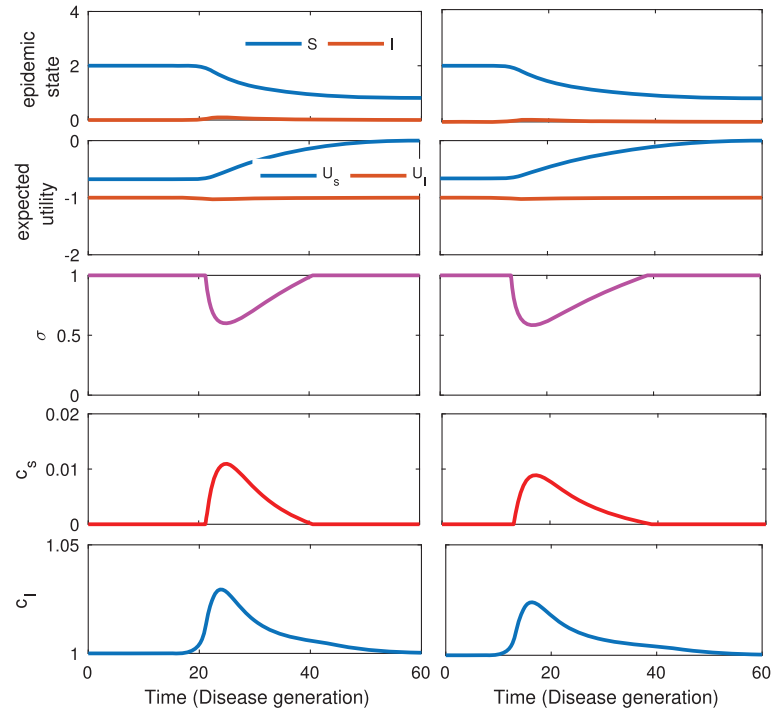

FIG. 9. Equilibrium solutions of social distancing with linear cost of infection $c_I = 1 + bI$, $b = 0.3$: Left panel exhibits figures with $m = 60$ and right panel denotes figures with $m = 80$. There is always positive social distancing when cost of infection increases with incidence I. Note that the social distancing behaviour is biphasic when b is negative (Fig. 4).

COI per generation, so an individual invests low cost in social distancing altogether, but it emerges much before and prolongs to the end of outbreak as efficiency of social distancing increases (Fig. 9).

(ii) Cost of infection $c_I = \exp(rI)$

With the exponential cost function, we have

$$\text{COI per generation} = \frac{c_I}{m} = \frac{1}{m}\exp(rI) = \left(\frac{1}{m} + \frac{r}{m}I\right) + \frac{r^2I^2}{m}\left[\frac{1}{2!} + \frac{rI}{3!} + \frac{r^2I^2}{4!}\ldots\right]. \tag{4.2}$$

So, the COI per generation with exponential function in (4.2) has a much larger effect of disease incidence I and the coefficient $r(< 0)$, compare to the linear case in (4.1) with $b < 0$. We simulate the model for different values of maximum efficiency m of social distancing, and $r = -0.8$ (Fig. 10). As the figure shows, the qualitative dynamics is similar to the linear case (Fig. 4), but the cost invested c_S for the same amount of social distancing is much larger when the cost of incidence c_I is exponential (compare fourth panel from top of Figs 10 and 4). A similar observation is found when the model is simulated for different values of r (< 0) in (4.2) (Fig. 11). The COI per generation in (4.2) always increases if $r > 0$. Even a small positive value of r increases the COI in such a high level that scalar root does not exist, while we simulate of the model system (2.8) under the chosen parameter values and initial conditions such as $S(0) = R_0 = 4$. In fact, the utility U_S of being susceptible is much lower than the utility U_I

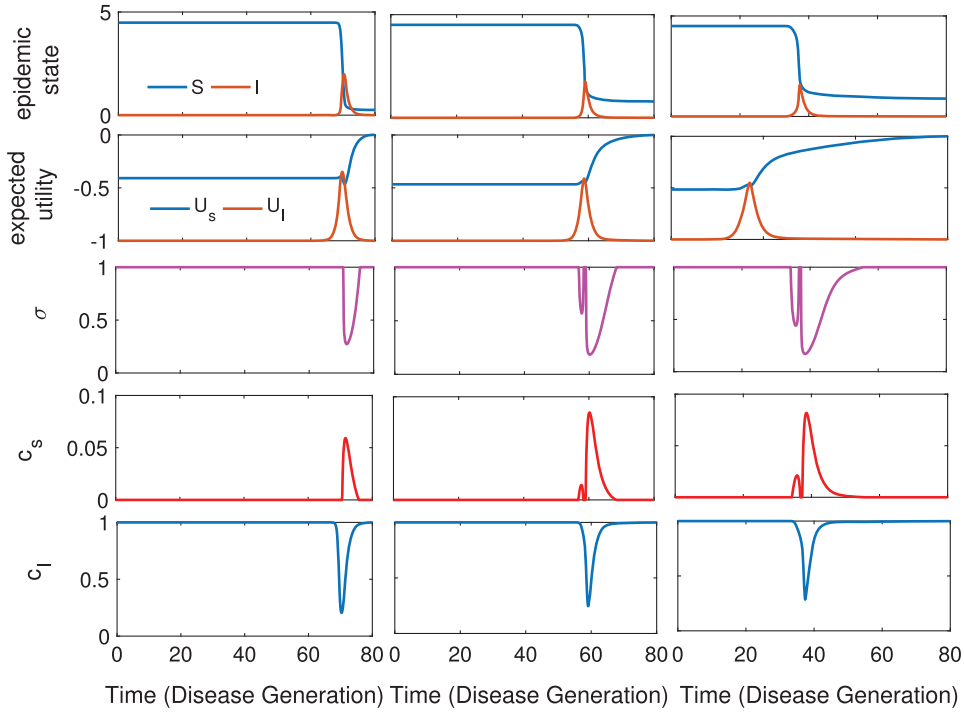

FIG. 10. Equilibrium solutions of social distancing when the cost function of infection is (ii) $c_I(I) = \exp(rI)$, $r = -0.8$. Plots are shown for three different values of social distancing efficiency: left panel exhibits figures with $m = 45$, middle panel with $m = 105$ and right panel denotes figures with $m = 150$. Unlike the linear cost function (i) (Fig. 4), efficiency m does not have much impact on the amount of social distancing (indicated by the area under the red curve in third horizontal panel from the top). Also, the epidemic cost $U_S(0)$ is higher compared to the linear cost function (Fig. 4).

of being infected due to very high COI per generation and so there does not exist any positive c_s^* for equilibrium social distancing (see (3.4)). The scaler root certainly exists at higher R_0, but this may not be very realistic case as we consider here.

(iii) Cost of infection $c_I = 1 + \frac{bI}{k+I}$

With this cost function, we have

$$\text{COI per generation} = \frac{c_I}{m} = \frac{1}{m} + \frac{b}{m}\frac{I}{k+I} = \left(\frac{1}{m} + \frac{b}{mk}I\right) - \frac{bI^2}{mk^2}\left[1 - \frac{I}{k} + \frac{I^2}{k^2}\cdots\right]. \tag{4.3}$$

The COI per generation in (4.3) changes in a non-linear way depending on the disease incidence I in the population. In fact, it increases or decreases relatively at a higher rate for a lower value of k, when $b > 0$ or $b < 0$, respectively. We simulate the model considering moderate value of $k = 5$. As seen in Fig. 12, system behaves qualitatively similar to the linear cost function. The equilibrium social distancing is biphasic when $b < 0$, i.e. individuals involved in social distancing in the beginning and end of the outbreak, but however, there is always social distancing when $b > 0$ (right panel of Fig. 12).

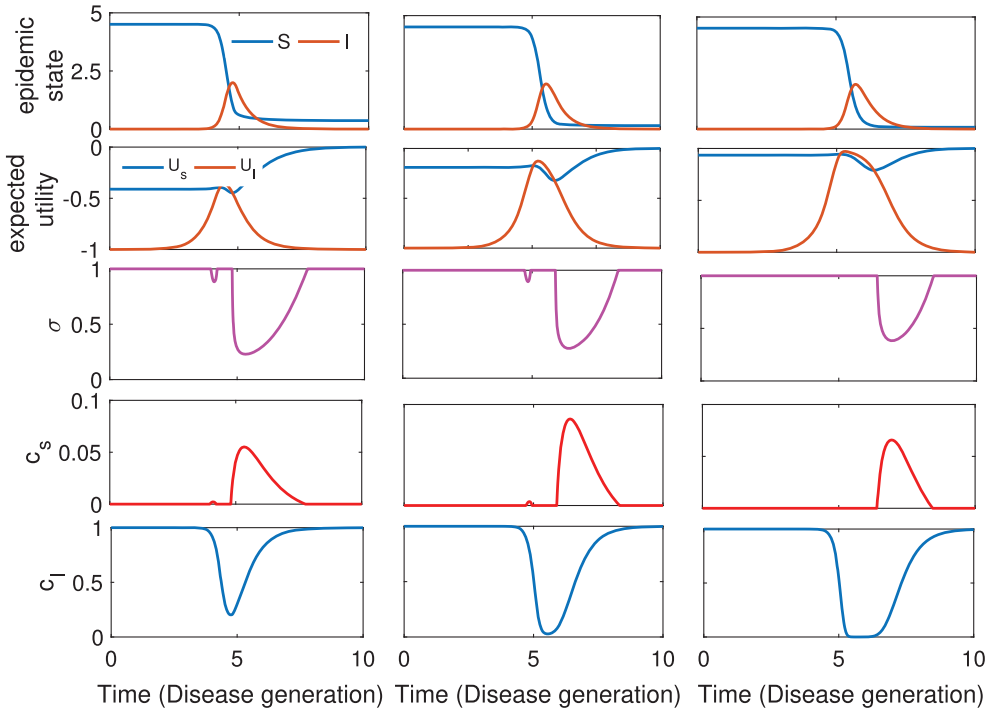

FIG. 11. Equilibrium solutions of social distancing when cost function of infection is (ii) $c_I(I) = \exp(rI)$, $r < 0$ and efficiency $m = 45$. Plots are shown for three different values of r: left panel exhibits figures with $r = -0.8$, middle panel with $r = -1.8$ and right panel denotes figures with $r = -4.8$. With higher magnitude of r (from left to right of the third horizontal panel) the social distancing decreases, as the cost of incidence decreases. Also, the epidemic cost $-U_S(0)$ in the expected utility decreases with lower values of r.

The most interesting observation with this non-linear cost function is that the onset of the emergence of social distancing for different values of k. We consider different values of k implying rapid to slower decline of COI per generation in (4.3) (Fig. 13(a)). As seen in Fig. 13(b), increase in k advances the emergence of social distancing and prolongs during the outbreak, while it shows more biphasic pattern for lower values of k. With lower values of k, the COI per generation in (4.3) decreases in such a low value that there is no initiative for social distancing; whereas at higher values of k, there is not much reduction in the COI and hence individuals initiate social distancing as early as possible. Thus, non-linearity of the cost function has impact on the emergence of social distancing behaviour in the population.

5. Discussion

Social distancing is an important aspect of public heath measures in mitigating the spread of infectious disease. But, the success of this isolation mechanism depends on how individuals respond to it. Previous works have demonstrated how an interplay between cost and benefit of social distancing in the face of an outbreak can reduce the contacts and impact the disease dynamics (Reluga, 2010, 2013). However, most of the earlier works assume that the perceived cost of infection is constant during the entire outbreak,

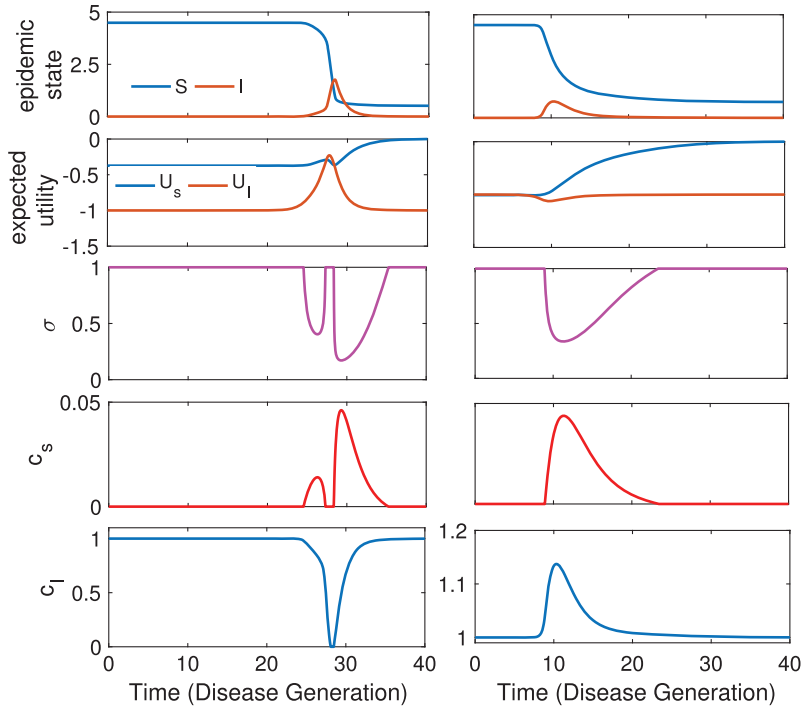

FIG. 12. Time series plot of model equations (2.8) showing equilibrium solutions for cost function (iii) $c_I(I) = 1 + \frac{bI}{k+I}$, $k = 5$: Left panel exhibits figures with $b = -1$ and right panel denotes figures with $b = 1$. The other parameter values considered in the simulation are $m = 45$, $R_0 = 4.5$. As the figure shows, when the cost of infection decreases the social distancing behaviour may exhibit biphasic pattern, whereas there is always a positive social distancing during the outbreak when b is positive.

which may not be very realistic. In a realistic scenario, the perceived cost of infection is closely related to the availability of vaccines, treatment cost and facilities and disease management systems, and thus actually evolves with the burden of epidemic.

Here in this paper we frame the individual decision process of social distancing during an outbreak as a differential population game and find the equilibrium social distancing as a subgame perfect Nash equilibrium of the original game. A Nash equilibrium strategy is a subgame perfect equilibrium if it is also a Nash equilibrium at every state the system may pass through. We implement a greedy algorithm (Isaacs, 1999) at every step in the game and find the investment in social distancing that maximizes the rate of increase in the individual's expected value U_S, or in turn, that minimizes the cost c_S of social distancing. We assume that the cost of infection is a function of the disease burden, and hence an implicit function of time. We explore with linear and different non-linear functions and compute the Nash equilibrium social distancing under different parametric conditions. We see that the Nash equilibrium cost of social distancing is a function of the expected utility of susceptible, utility of infected and the disease incidence. The dynamics of social distancing and disease prevalence in the population depend on two key parameters: the efficiency of social distancing and the propensity at which the cost of infection changes with the disease prevalence. Obviously, the basic reproduction rate plays a major role in describing the disease process.

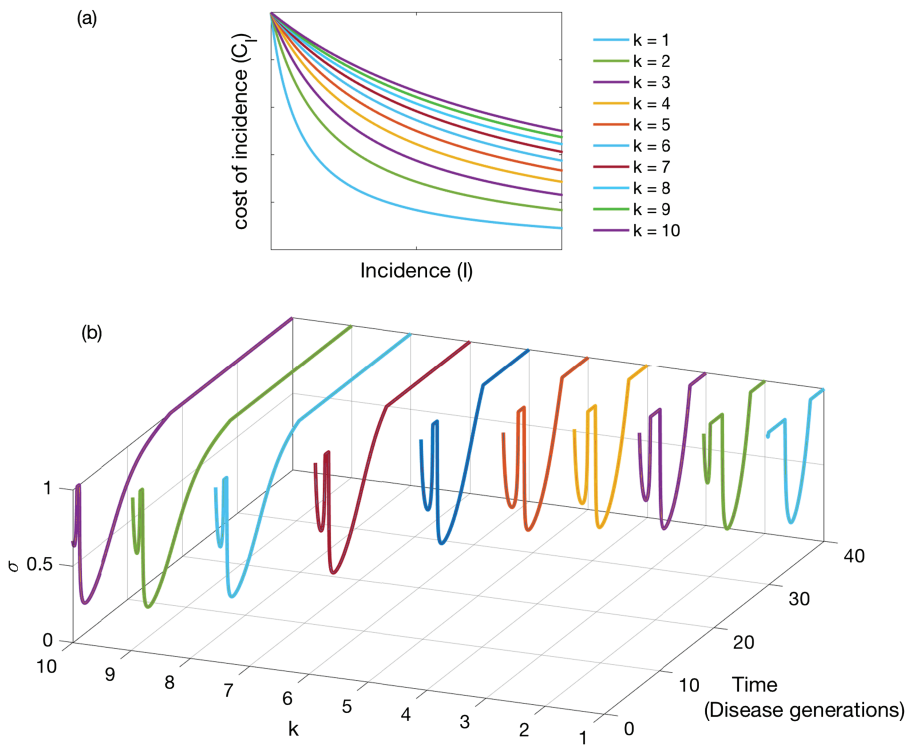

FIG. 13. Dynamics of social distancing at different values of k for the non-linear cost function (iii) $c_I = 1 + \frac{bI}{k+I}, b = -1$. The efficiency of social distancing $m = 45$ and $R_0 = 4.5$. Fig. (a) shows the cost of infection $c_I(I)$ for different values of k (all curves starts from same $c_I = 1$), and Fig. (b) shows the equilibrium social distancing at different values of k in the cost of infection. Increase in k advances the emergence of social distancing and prolongs to the end of outbreak, while it shows more biphasic pattern for lower values of k. With lower values of k, the cost of infection c_I decreases in such a low values, so that there is no initiative for social distancing, whereas in higher values of there is not much reduction in the c_I and hence individuals initiate social distancing as early as possible.

In a scenario, where the cost of infection linearly decreases with disease incidence, we show that the individual involvement in social distancing increases with the increase in efficiency of the isolation mechanism, and the equilibrium behaviour is to concentrate on social distancing effort at the beginning and the end of the epidemic outbreak that leads to an epidemic with lower outbreak size. In contrast, social distancing decreases with the increase in the linear slope of the cost function. The slope of the cost function determines how rapid the cost of infection per generation changes with the infected population density and so is the incentive of individual investment in social distancing.

The consequence of social distancing are also portrayed in Figs 6 and 7. The per capita cost of epidemic is high with higher basic reproduction numbers. But with more efficient social distancing (determined by m) and rapid decline of cost function (determined by b), the more of the epidemic cost can be saved per person. In certain parameter regimes, our game dynamic model also exhibits multiple waves of epidemic outbreak. It has been shown earlier that the social isolation can generate multiple waves in pandemic influenza (Caley *et al.*, 2008). This work exemplifies this phenomenon to some extent at the higher efficiency of the isolation mechanism.

We have only computed the Nash equilibrium strategy from our dynamic game model. But there are other important solution concepts in the social distancing game, like strict Nash equilibria and Nash equilibria with invasion potential or evolutionary stable strategy, which can be computed directly from the utility function at the stationary solution of population model (Reluga & Galvani, 2011). However, we consider a single outbreak of influenza rather than an endemic disease such as measles. So, we have analysed the dynamics of social distancing over a finite period of time and hence our present population model does not have any nontrivial stationary solution. Thus, we cannot compute the closed form of the utility functions and other equilibrium solutions in the current form of the social distancing model.

Model predictions may also vary if we incorporate other factors in our model system. For example, we have considered simple SIR model describing the homogeneous mixing of populations. Age-stratified contact structures among individuals in a population not only affect the disease progression [Meyers *et al*. (2006); Meyers (2007)], but also influence the individual strategy in social distancing by the clustered information on disease and the cost of infection. In our model, we have considered hyperbolic function to represent the reduction of transmission due to social distancing. Model predictions may also vary if we consider other efficacy functions representing social distancing, e.g. piecewise convex functions. Reluga (2013) has explored similar possibilities with piecewise linear and linear social distancing cost functions. Other realistic characteristics such as particular infectious disease, stochasticity in spread of infection, arbitrary infectious period or even incomplete information about the epidemic may influence the results. There is also an open question such as how the equilibrium strategies evolve, if vaccines are available after some time of the emergence of outbreak. However, these possibilities suggest interesting areas for future research.

References

Anderson, R. M. & May, R. M. (1992) *Infectious Diseases of Humans: Dynamics and Control*. New York: Oxford University Press.

Bauch, C. T. & Bhattacharyya, S. (2012) Evolutionary game theory and social learning can determine how vaccine scares unfold. *PLoS Comput. Biol.*, **8**, e1002452.

Bhattacharyya, S. & Bauch, C. (2010) A game dynamic model for delayer strategies in vaccinating behaviour for pediatric infectious diseases. *J. Theor. Biol.*, **267**, 276–282.

Bhattacharyya, S. & Bauch, C. T. (2011) "Wait and see" vaccinating behaviour during a pandemic: a game theoretic analysis. *Vaccine*, **29**, 5519–5525.

Bhattacharyya, S., Bauch, C. T. & Breban, R. (2015) Role of word-of-mouth for programs of voluntary vaccination: a game-theoretic approach. *Math. Biosci.*, **269**, 130–134.

Buonomo, B., d'Onofrio, A. & Lacitignola, D. (2008) Global stability of an SIR epidemic model with information dependent vaccination. *Math. Biosci.*, **216**, 9–16.

Caley, P., Philp, D. J. & McCracken, K. (2008) Quantifying social distancing arising from pandemic influenza. *J. R. Soc. Interface*, **5**, 631–639.

Chen, F., Jiang, M., Rabidoux, S. & Robinson, S. (2011) Public avoidance and epidemics: insights from an economic model. *J. Theor. Biol.*, **278**, 107–119.

Chen, F. H. (2006) On the transmission of HIV with self-protective behavior and preferred mixing. *Math. Biosci.*, **199**, 141–159.

Chen, F. H. (2009) Modeling the effect of information quality on risk behavior change and the transmission of infectious diseases. *Math. Biosci.*, **217**, 125–133.

Del Valle, S., Hethcote, H., Hyman, J. M. & Castillo-Chavez, C. (2005) Effects of behavioral changes in a smallpox attack model. *Math. Biosci.*, **195**, 228–251.

Funk, S., Salathé, M. & Jansen, V. A. (2010) Modelling the influence of human behaviour on the spread of infectious diseases: a review. *J. R. Soc. Interface*, **7**, 1247–1256.

Glass, R. J., Glass, L. M., Beyeler, W. E. & Min, H. J. et al. (2006) Targeted social distancing design for pandemic influenza. *Emerg. Infect. Dis.*, **12**, 1671–1681.

Isaacs, R. (1999) *Differential Games: A Mathematical Theory with Applications to Warfare and Pursuit, Control and Optimization*. Mineola, New York: Courier Corporation.

Kelso, J. K., Milne, G. J. & Kelly, H. (2009) Simulation suggests that rapid activation of social distancing can arrest epidemic development due to a novel strain of influenza. *BMC Public Health*, **9**, 1.

Lenhart, S. & Workman, J. T. (2007) *Optimal Control Applied to Biological Models*. CRC Press.

Meyers, L. (2007) Contact network epidemiology: bond percolation applied to infectious disease prediction and control. *Bull. Am. Math. Soc.*, **44**, 63–86.

Meyers, L. A., Newman, M. & Pourbohloul, B. (2006) Predicting epidemics on directed contact networks. *J. Theor. Biol.*, **240**, 400–418.

d'Onofrio, A. & Manfredi, P. (2009) Information-related changes in contact patterns may trigger oscillations in the endemic prevalence of infectious diseases. *J. Theor. Biol.*, **256**, 473–478.

Osborne, J. M. (2004) *An Introduction to Game Theory*. Oxford University Press.

Reluga, T. C. (2010) Game theory of social distancing in response to an epidemic. *PLoS Comput. Biol.*, **6**, e1000793.

Reluga, T. C. (2013) Equilibria of an epidemic game with piecewise linear social distancing cost. *Bull. Math. Biol.*, **75**, 1961–1984.

Reluga, T. C., Bauch, C. T. & Galvani, A. P. (2006) Evolving public perceptions and stability in vaccine uptake. *Math. Biosci.*, **204**, 185–198.

Reluga, T. C. & Galvani, A. P. (2011) A general approach for population games with application to vaccination. *Math. Biosci.*, **230**, 67–78.

Valdez, L., Buono, C., Macri, P. & Braunstein, L. (2013) Social distancing strategies against disease spreading. *Fractals*, **21**, 1350019.

Valdez, L., Macri, P. A. & Braunstein, L. A. (2012) Intermittent social distancing strategy for epidemic control. *Phys. Rev. E*, **85**, 036108.